Quantifying the artefacts caused by hyperoxic challenges

I. Driver[1], J. Harmer[1], E. Hall[1], S. Pritchard[1], S. Francis[1], and P. Gowland[1]
[1]Sir Peter Mansfield Magnetic Resonance Centre, University of Nottingham, Nottingham, United Kingdom

Introduction Hyperoxia (which leads to increased venous oxygen saturation (1) and a positive BOLD signal) has been used both to estimate cerebral blood volume (2) and for BOLD calibration (3). However, an increase in inspired oxygen fraction will increase the tissue-air susceptibility close to the oral cavity and sinuses, due to the paramagnetic nature of oxygen, causing a global field inhomogeneity. This effect has been observed as a decreased signal under hyperoxia (4,5). It is therefore important to map the effect of hyperoxia on the magnetic field homogeneity within the brain, and account for both the changes in transverse relaxation rate (R_2*) and image distortions induced. This study considers the quantitative effect of hyperoxia on image acquisition.

Methods 5 healthy volunteers (3 male, 2 female, aged 25±3 years) were scanned using a Philips Achieva 7T system with volume transmit and 16-channel head receive coil. The study was approved by the local ethics committee and written informed consent was obtained prior to scanning. End-tidal O_2 ($P_{ET}O_2$) and CO_2 ($P_{ET}CO_2$) partial pressures were controlled and monitored using a sequential gas delivery breathing circuit and a prospective, feed-forward gas delivery system (Respiract™, Thornhill Research Inc., Toronto, Canada). Targeted $P_{ET}O_2$ was modulated between the subject's baseline value (~110 mmHg; normoxia) and 500 mmHg (hyperoxia), for two cycles of three minutes of normoxia followed by three minutes of hyperoxia, followed by a final three minute period of normoxia. Isocapnia was maintained at the subject's baseline (~40 mmHg $P_{ET}CO_2$). Gradient-echo EPI data (TE = 25ms, SENSE = 3, voxel band-width = 41.5Hz, 30 axial slices of 2 mm isotropic voxels spanning from the ventricles to the motor cortex in a TR = 2.4s) were acquired during the respiratory challenge, with magnitude and phase data saved. To map the underlying B_0 field, prior to the respiratory challenge GE-EPI data were acquired with the same parameters as above, but with TE = 25/28ms for alternate dynamics, with 10 averages of each collected. A 7th order three dimensional polynomial fit was applied to the resulting B_0 map to reduce the effects of noise and small scale variations due to vessels and grey/white matter contrast, whilst accurately modelling the large variation close to the frontal sinus. The series of phase images collected through the hyperoxic challenge were combined with the initial field measurement to form a time series of B_0 maps (6,7); maps of the field shift due to hyperoxia were formed by subtracting data from the average normoxic periods from averaged hyperoxic periods.

The EPI distortion due to hyperoxia was estimated by comparing the hyperoxia-induced field shift to the voxel bandwidth. The change in intravoxel spin de-phasing due to the change in field homogeneity was simulated. A 7th order, 3D polynomial was fitted to the hyperoxia-induced field shift map (Fig. 1a,b). Each voxel was subdivided into 10x10x10 spin isochromats and the polynomial fit coefficients were used to interpolate a value of frequency shift (Δf) for each isochromat. The phase of each isochromat was allowed to evolve over the echo time (TE) by $\phi = 2\pi\Delta f$TE. For each voxel, the phase of all isochromats were combined by vector summation to estimate intravoxel de-phasing. This provided a measure of signal attenuation due to the hyperoxia-induced change in field homogeneity across each voxel (Fig. 1c).

Results The frequency shift induced by hyperoxia is shown for a typical subject in Fig. 1a. The magnitude of this shift is largest in the frontal sinus, up to 20 Hz (50% of the voxel bandwidth) and declines with distance from the frontal sinus, but never drops to zero. Single-subject timecourses of the frequency shift from the frontal sinus (black), motor (blue) and visual cortices (green) are shown in Fig. 1e. The hyperoxia-induced frequency shift in 5x5 voxel ROIs in the motor (M1) and visual (V1) cortices (Fig. 1d), is 3.1±0.2 Hz in M1 and 2.1±0.7 Hz in V1 (mean±std over subjects), corresponding respectively to 7% and 5% of a voxel volume along the phase-encode direction. Fig. 1c shows the map of simulated signal attenuation due to field inhomogeneity for this subject. Simulations indicate that the change in field homogeneity due to hyperoxia will cause a signal attenuation of 8±9 x10^{-4} % in M1 and 4±4 x10^{-4} % in V1 (mean± std over subjects).

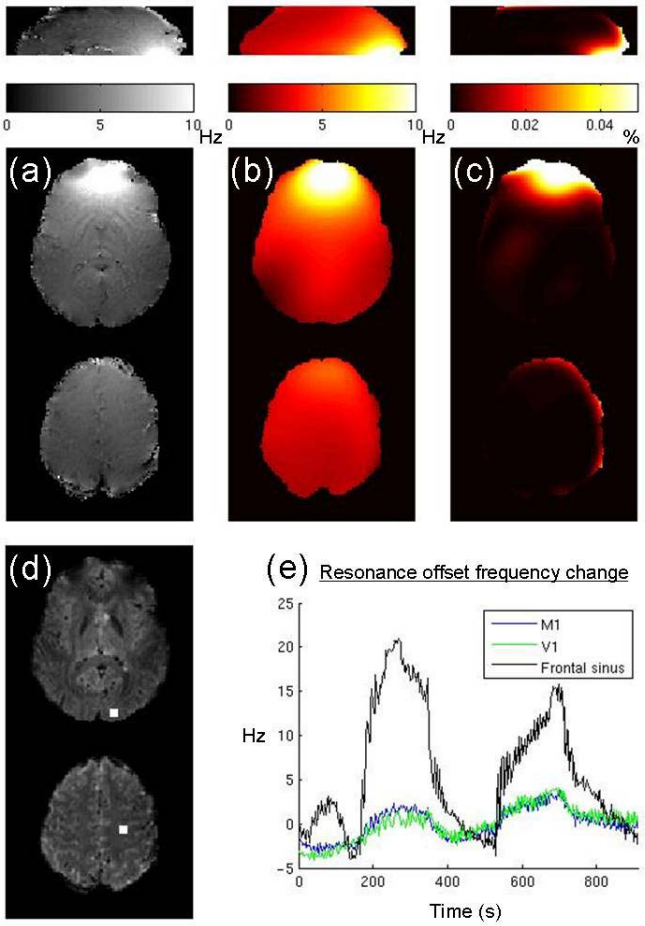

Figure 1: Single subject (a) Map of resonance offset change (in Hz) due to hyperoxia (1 sagittal and 2 axial slices); (b) Polynomial fit to (a); (c) Map of simulated signal attenuation (%) due to hyperoxic changes in field homogeneity; (d) The location of the 5x5 voxel V1 and M1 ROIs; (e) Timecourses of frequency shift during the 15 minute hyperoxia paradigm, taken from maps of frequency shift (a). M1, V1 ROIs together with an ROI from the frontal sinus shown.

Discussion The field shift due to oxygen in the sinuses extended over the whole head, but the resulting change in intravoxel dephasing did not significantly change the transverse relaxation rate (<0.05%) apart from in voxels neighbouring the frontal sinus. There was, however a significant change in the EPI distortions due to this field shift, which will lead to the voxel composition changing under hyperoxia (by 7% in M1 and 5% in V1) in the phase-encode direction. Dynamic distortion correction techniques may be able to compensate for this. Our analysis assumed that the effect of oxygen in the sinuses could be modelled using a 7th order polynomial, based on evidence from the field of respiration-induced resonance offsets (8), and this was found to be reasonable, except for in some deep grey matter regions (Fig 1a). Previous studies (5,9) have also mapped the change in B_0 due to hyperoxia. These studies showed a large effect in the frontal sinus, but did not quantify the effects in other regions away from the frontal sinus and of interest for many fMRI experiments. In conclusion, the hyperoxia-induced artefacts due to oxygen in the sinuses or oral cavity will not significantly contaminate results of calibrated BOLD or CBV measurements made using hyperoxia, although small shifts in voxel position must be considered. The technique described here should be used with any hyperoxia study to monitor the temporal variations in B_0 induced by hyperoxia.

References: (1) Rostrup, NMR in Biomedicine 8:41, 1995; (2) Bulte, JMRI 26:894, 2007; (3) Chiarelli, NeuroImage 37:808, 2007; (4) Blockley, Proc. ISMRM 17:1618, 2009; (5) Pilkington, Proc. ISMRM 18:3482, 2010; (6) Hahn, NeuroImage 44:742, 2009; (7) Lamberton, JMRI 26:747, 2007; (8) Van de Moortele MRM 47:888, 2002; (9) Marques Proc. ISMRM 18:3015, 2010. **Acknowledgement:** Funded by the UK Medical Research Council